Synthesis, Crystal Structure, Electrochemistry and Molecular-orbital Analysis of the Piano-stool Dimer $[Mo_2(\eta\text{-}C_5H_5)_2(CO)_4(NC_5H_4PPh_2\text{-}2)_2]$ *

Carmela G. Arena,[a] Felice Faraone,[a] Marco Fochi,[b] Maurizio Lanfranchi,[c] Carlo Mealli,[b] Renato Seeber[d] and Antonio Tiripicchio[c]

[a] *Dipartimento di Chimica Inorganica e Struttura Molecolare, Universita di Messina, Salita Sperone 31, Villaggio S. Agata, I-98010 Messina, Italy*

[b] *Istituto per lo Studio della Stereochimica ed Energetica dei Composti di Coordinazione, C.N.R., Via J. Nardi 39, I-50132 Firenze, Italy*

[c] *Istituto di Chimica Generale ed Inorganica, Università di Parma, Centro di Studio per la Strutturistica Diffrattometrica del C.N.R., Viale delle Scienze 78, I-43100 Parma, Italy*

[d] *Dipartimento di Chimica, Università di Sassari, Via Vienna, I-07100 Sassari, Italy*

The addition of 2-(diphenylphosphino)pyridine ($NC_5H_4PPh_2$-2) to an *in situ* prepared *m*-xylene solution of $[Mo_2(\eta\text{-}C_5H_5)_2(CO)_4]$ (molar ratio 2:1), at room temperature, yields the complex $[Mo_2(\eta\text{-}C_5H_5)_2(CO)_4(NC_5H_4PPh_2\text{-}2)_2]$ **1**. Compound **1** is easily converted into the cationic molybdenum(II) mononuclear complex $[Mo(\eta\text{-}C_5H_5)(CO)_3(NC_5H_4PPh_2\text{-}2)]PF_6$ **2** by reaction with $AgPF_6$. Reduction of **1** with Na or Na/Hg, in tetrahydrofuran, affords an air-sensitive solution containing $Na[Mo(\eta\text{-}C_5H_5)(CO)_2(NC_5H_4PPh_2\text{-}2)]$ **3**, together with minor products. Electrochemical measurements show that **1** undergoes a reversible one-electron oxidation followed by relatively slow decomposition of the electrogenerated species. The molecular structure of the diethyl ether solvate of **1** was determined by X-ray diffraction methods: monoclinic, space group $P2_1/c$, with $a = 13.218(4)$, $b = 19.485(6)$, $c = 11.019(4)$ Å, $\beta = 110.10(2)°$ and $Z = 2$. The centrosymmetric complex **1** is a typical piano-stool dimer in which two units share the leg coinciding with the Mo–Mo vector. Similarly to other compounds of this type, the M–M separation is quite long [Mo–Mo 3.276(3) Å], *ca.* 0.5 Å longer than the sum of the metal radii. The evidence for the single metal–metal bond (predicted by counting rules) and its role in providing the system's stability is discussed in terms of qualitative molecular orbital theory. The extended-Hückel method used appears sufficiently reliable as the total electronic energy minimizes for an intermetal separation close to the experimental one. The loss of σ bonding, on elongating Mo–Mo, is counterbalanced by the diminished repulsion between metal lone pairs (filled *xy* orbitals), thus the intermetallic distance is an evident compromise between attractive and repulsive electronic forces. Steric factors may not be so important. The theoretical implications for the eventual homolytic cleavage of the dimer are also underlined. A rationale is provided for the effects that follow the removal of one electron from the system.

Interest in the chemistry of homo- and hetero- bi- and polynuclear complexes (most often supported by the presence of short-bite bridging ligands which favour by their nature direct metal–metal interactions) caused some of us to study the reaction of $[Mo_2(\eta\text{-}C_5H_5)_2(CO)_4]$[1] with 2-(diphenylphosphino)pyridine ($NC_5H_4PPh_2$-2).[2–6] The bimetallic precursor readily undergoes nucleophilic addition at the Mo≡Mo triple bond, and the product obtained in this case, $[M_2(\eta\text{-}C_5H_5)_2(CO)_4(NC_5H_4PPh_2\text{-}2)_2]$ **1**, is a piano-stool dimer not dissimilar from others containing phosphines such as PPh_3 or phosphites such as $P(OMe)_3$.[7–9] All of the latter complexes can be considered derivatives of the well known series $[Mo_2(\eta\text{-}C_5H_5)_2(CO)_6]$ (M = Cr, Mo or W).[10] The full characterization of **1**, including its crystal structure and electrochemical measurements, revives old curiosities, never entirely satisfied, about the structural and electronic properties of this type of unbridged piano-stool dimer. The outstanding feature is the long M–M separation (*ca.* 3.2–3.3 Å) to which the simplest electron-counting ideas assign the bond order of one. Can the apparently weak interaction between the metals provide the necessary stability to the dimeric aggregate? What is the relative importance of steric and electronic factors? In this paper we attempt to give a reasonable answer to these questions by using a pictorial molecular orbital (MO) approach[11] based on extended-Hückel molecular orbital (EHMO) calculations[12] with frontier molecular orbital (FMO) analysis.[13]

* *Supplementary data available:* see Instructions for Authors, *J. Chem. Soc., Dalton Trans.*, 1992, Issue 1. pp. xx–xxv.

Non-SI unit employed: eV ≈ 1.60×10^{-19} J.

Results and Discussion

Synthesis and Redox Properties of $[Mo_2(\eta\text{-}C_5H_5)_2(CO)_4(NC_5H_4PPh_2\text{-}2)_2]$ **1**.—The addition of $NC_5H_4PPh_2$-2 to a *m*-xylene solution of $[Mo_2(\eta\text{-}C_5H_5)_2(CO_4)]$ {prepared *in situ* by refluxing for several hours a *m*-xylene solution of $[Mo_2(\eta\text{-}C_5H_5)_2(CO)_6]$[14]}, in the molar ratio 2:1, afforded, after addition of light petroleum (b.p. 40–60 °C), the product $[Mo_2(\eta\text{-}C_5H_5)_2(CO)_4(NC_5H_4PPh_2\text{-}2)_2]$ **1** as red-purple crystals in high yield. Formation of a product different from **1** was not observed even when an equimolar ratio was used, this behaviour indicating that the formation of a compound in which the $NC_5H_4PPh_2$-2 bridges the Mo atoms is to be

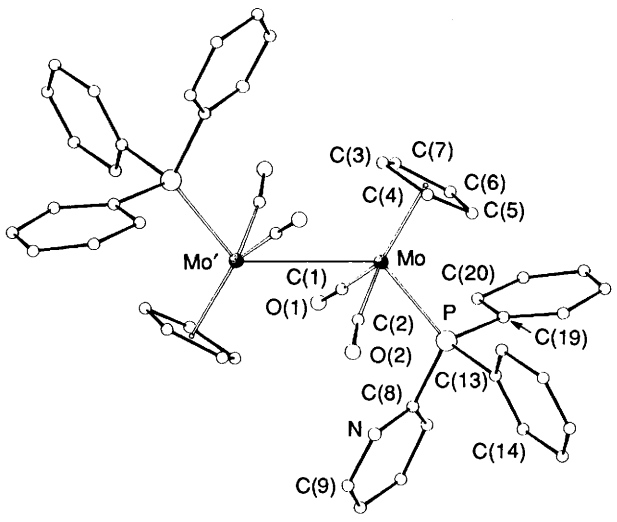

Fig. 1 View of the molecular structure of $[Mo_2(\eta\text{-}C_5H_5)_2(CO)_4(NC_5H_4PPh_2\text{-}2)_2]$ **1** with the atomic numbering scheme

Table 1 Selected bond distances (Å) and angles (°) in complex **1***

Mo–Mo′	3.276(3)	P–C(13)	1.84(3)
Mo–P	2.412(6)	P–C(19)	1.83(2)
Mo–C(1)	1.96(2)	N–C(8)	1.33(3)
Mo–C(2)	1.96(2)	N–C(9)	1.35(3)
Mo–C(3)	2.39(2)	C(1)–O(1)	1.16(3)
Mo–C(4)	2.34(3)	C(2)–O(2)	1.16(3)
Mo–C(5)	2.35(3)	C(3)–C(4)	1.39(5)
Mo–C(6)	2.33(2)	C(4)–C(5)	1.46(3)
Mo–C(7)	2.33(3)	C(5)–C(6)	1.41(5)
Mo–CE	2.02(2)	C(6)–C(7)	1.37(4)
P–C(8)	1.83(2)	C(3)–C(7)	1.44(5)
Mo′–Mo–C(1)	73.6(5)	Mo–P–C(8)	118.4(8)
C(1)–Mo–P	78.8(6)	Mo–P–C(13)	120.3(6)
C(2)–Mo–P	80.6(6)	Mo–P–C(19)	112.1(6)
Mo′–Mo–C(2)	68.6(7)	C(8)–P–C(13)	99.3(9)
CE–Mo–Mo′	116.6(8)	C(8)–P–C(19)	104.3(9)
CE–Mo–P	112.8(9)	C(13)–P–C(19)	99.7(10)
CE–Mo–C(1)	126.3(10)	Mo–C(1)–O(1)	177(2)
CE–Mo–C(2)	128.2(10)	Mo–C(2)–O(2)	170(2)

* CE is the centroid of the cyclopentadienyl ring. The primed atoms are related to the unprimed ones by the transformation $-x, -y, -z$.

excluded. Compound **1** easily dissolves in dichloromethane and, to a lesser extent, in benzene and diethyl ether, the solutions being air-sensitive.

The IR spectrum of compound **1** (Nujol mull) shows a single terminal ν(CO) band at 1833 cm^{-1} indicating a symmetric structure. The ^1H NMR spectrum, in $CDCl_3$ solution, exhibits the cyclopentadienyl resonance at δ 4.62; the ratio of the cyclopentadienyl and $NC_5H_4PPh_2$-2 protons indicates the incorporation of two phosphine ligands into the dinuclear molecule. The *ortho*-hydrogen of the pyridine ring gives a distinct resonance at δ 8.77 characteristic of an unco-ordinated pyridine nitrogen atom (when the latter atom is co-ordinated the *o*-hydrogen resonance is usually shifted to higher frequency).[4,5] The moderate solubility and stability of **1** in CH_2Cl_2 prevented measurements of reliable $^{31}P\text{-}\{^1H\}$ NMR spectra.

The addition of 2 equivalents of $AgPF_6$ to compound **1** in CH_2Cl_2 gave slow deposition of silver metal and a brown-orange solution from which the diamagnetic complex $[Mo_2(\eta\text{-}C_5H_5)(CO)_3(NC_5H_4PPh_2\text{-}2)]PF_6$ **2** was isolated as a yellow-orange solid; the salt was characterized by elemental analysis, conductivity measurements and by IR and NMR spectroscopy. The carbonyl stretching bands [ν(CO) 2066, 1973 and 1908 cm^{-1} (Nujol mull)] are at higher wavenumber than that of complex **1**. The feature is consistent with the oxidation of the molybdenum centre and the positive charge. In accordance, the ^1H NMR ($CDCl_3$) spectrum displays the cyclopentadienyl resonance at higher δ (5.21) than for **1**; the *o*-hydrogen of the pyridine ring gives a resonance at δ 8.99 indicating that the pyridine nitrogen atom is unco-ordinated. In the $^{31}P\text{-}\{^1H\}$ NMR spectrum ($CDCl_3$), at 260 K, the P resonance of $NC_5H_4PPh_2$-2 was observed as a singlet at δ 58.0. The high-frequency chemical shift is consistent with a structure in which the $NC_5H_4PPh_2$-2 ligand is P bonded; a large upfield shift would be expected if the ligand were acting as a chelate in which the P atom is part of a four-membered ring.[5]

Reduction of compound **1** with Na/Hg or Na in tetrahydrofuran (thf) solution provided a yellow, air-sensitive solution containing $Na[Mo(\eta\text{-}C_5H_5)(CO)_2(NC_5H_4PPh_2\text{-}2)]$ **3**, as well as other minor products. The use of other solvents, such as 1,2-dimethoxyethane, did not give better results. Compound **3** was detected by IR spectroscopy in thf solution [ν(CO) 1941 and 1900 cm^{-1}]; attempts to obtain it in a pure form also failed when a bulk precipitating cation was used.

Crystal Structure of $[Mo_2(\eta\text{-}C_5H_5)_2(CO)_4(NC_5H_4PPh_2\text{-}2)_2]\cdot 2OEt_2$ **1**.—In the crystals of compound **1** dimeric $[Mo_2(\eta\text{-}C_5H_5)_2(CO)_4(NC_5H_4PPh_2\text{-}2)_2]$ and diethyl ether molecules of solvation are present (Fig. 1). Selected bond distances and angles are given in Table 1. The complex **1** can be described as a typical piano-stool dimer in which two facing units, short of one terminal ligand, share the stool leg represented by the metal–metal linkage itself. The remaining three basal positions are occupied by two CO groups and by the P atom from one $NC_5H_4PPh_2$-2 molecule acting as a monodentate ligand [Mo–C 1.96(2) and Mo–P 2.412(6) Å]. The angles between adjacent legs range from 68.6(7) to 80.6(6)°, while the angles between the Mo–CE vector (CE is the cyclopentadienyl centroid) and the legs are in the range 112.8(9)–128.2(10)°. The Mo–CE distance is 2.02(2) Å. The dimeric complex has a crystallographically imposed C_i symmetry, and higher pseudo-symmetry, C_{2h}. Although the M–M bond order is assumed equal to one, here and in the very comparable dimer $[Mo_2(\eta\text{-}C_5H_5)_2(CO)_6]$ **4**,[10d] the Mo–Mo separation [3.276(3) and 3.235(1) Å, in **1** and **4** respectively] is *ca.* 0.5 Å longer than the sum of the metal radii.[15] Other strained M–M single bonds are found in $[M_2(CO)_{10}]$ dimers (M = Mn or Re). For example, in $[Mn_2(CO)_{10}]$ the intermetallic separation of 2.903 8(6) Å (room temperature)[16,*] is *ca.* 0.2 Å longer than the sum of the manganese radii. In $M_2(\eta\text{-}C_5H_5)_2L_6$ compounds the crowding of the ligands at each metal could suggest that the steric hindrance is an important factor against large metal–metal overlap. It is worth mentioning, in this respect, that the shortest contact of 2.85(3) Å, between the two $M(C_5H_5)L_3$ moieties in **1**, involves the C(1) and C(2) atoms of the co-ordinated CO ligands (compare with the analogous value of 2.81 Å observed in **4**). Although the steric factor cannot be undervalued, it will be shown later (see below) that repulsive electronic factors, in conflict but still not removing the direct Mo–Mo attraction, are at work in these structures.

Recently all of the known structures of piano-stool monomers have been examined statistically by Poli[17] who noticed how the angle θ formed at the metal by any of the terminal ligands (stool legs) and the CE seems to be a variable dependent on the π-bonding capabilities of the coligands. Moreover the θ angles, for pairs of *trans* ligands, are reciprocally affected (*trans* influence). By considering **1** as a $M(C_5H_5)L_4$ monomer in which a ligand is substituted by a second $Mo(C_5H_5)L_3$ moiety, the three different types of θ have values 127(1)° (average) for CE–Mo–C(O), 112.8(9)° for CE–Mo–P and 116.6(8)° for CE–Mo–Mo′, respectively. The phosphine ligand, usually

* 2.895(1) Å at 74 K.[16]

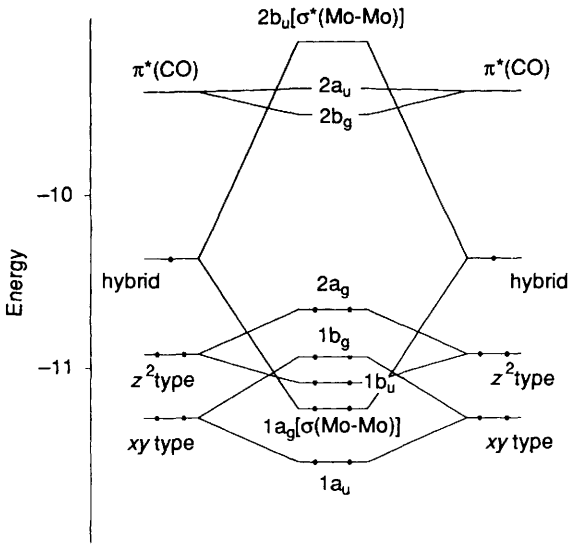

Fig. 2 Diagram for the interaction of two $Mo(C_5H_5)(CO_2)(PH_3)$ fragments to give the molecular orbitals of the piano-stool dimeric model of compound **1**. Considering the C_{2h} symmetry, z coincides with the two-fold axis, while the x direction is fixed by the Mo–Mo vector. Energies on the vertical scale are in eV.

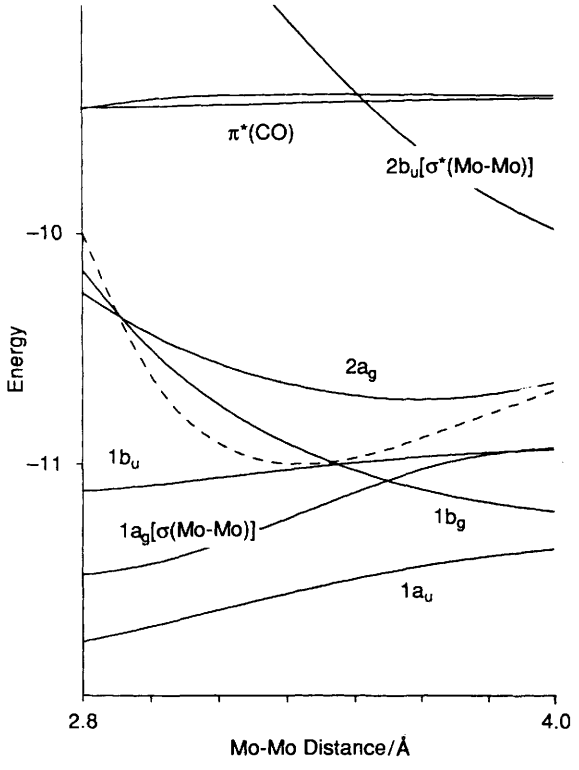

Fig. 3 Evolution of the frontier MOs and of the total energy (dashed line) for a model of the piano-stool dimer on elongating the Mo–Mo vector from 2.8 to 4.0 Å. The energies on the vertical axis are in eV, but, as far as the total energy is concerned, each division corresponds only to 0.5 eV on an independent, relative scale.

observed to induce large θ values, is in this case *trans*-influenced by the presence of the $Mo(C_5H_5)L_3$ fragment, that has no evident π-acceptor capabilities.

Electrochemistry of $[Mo_2(\eta\text{-}C_5H_5)_2(CO)_4(NC_5H_4PPh_2\text{-}2)_2]$ **1**.—Compound **1** is oxidized in a one-electron process, as inferred from cyclic voltammetric tests, which show an anodic peak (E_{pa} = +0.345 V at 0.5 V s^{-1} potential scan rate) with a directly associated backward cathodic response, and from controlled-potential coulometry at +0.5 V. Voltammograms, recorded after exhaustive electrolyses, reveal that the oxidation product directly formed at the electrode undergoes an irreversible chemical reaction, the cathodic–anodic peak system recorded on the starting solution now being absent. A different cathodic response (E_{pc} = −0.96 V) is detectable and can be attributed to reduction of the final product of the oxidation process.

The electrode oxidation of compound **1** should involve a reversible electrochemical–irreversible chemical mechanism since, by decreasing the potential scan rate, the ratio between the cathodic (backward) and anodic (forward) peak currents progressively lowers with respect to the unit value computed at 0.5 V s^{-1}. The response recorded at this potential scan rate is typical of an uncomplicated one-electron reversible charge transfer ($E_{pa} - E_{pc}$ = 60 mV; i_{pc}/i_{pa} = 1), so that an $E_{\frac{1}{2}}^{r}$ value of +0.315 V can be estimated for the formal Mo^{II}–Mo^{I}/Mo^{I}–Mo^{I} redox couple.[18] On the other hand, based on the values of i_{pc}/i_{pa} at different scan rates[19] and assuming a first-order decay, a value of 7.5 s can be computed for the half-life of the unstable electrogenerated Mo^{II}–Mo^{I} species. Unfortunately, any attempt to isolate a pure product from the oxidized solution failed. Ill defined, broad and poorly reproducible anodic peaks are also recorded at potentials more anodic than +1.2 V, on solutions of both the starting and the one-electron oxidized products.

Compound **1** undergoes irreversible reduction, as evidenced by cyclic voltammetry (E_{pc} = −1.40 V at 0.2 V s^{-1} potential scan rate). The current *vs.* potential curves do not show any reverse anodic peak directly associated with the cathodic response.

Electronic Features of $M_2(C_5H_5)_2L_6$ *Dimers and the Implications for the Nature of Metal–Metal Bonding*.—The $M_2(C_5H_5)_2L_6$ piano-stool dimers have been theoretically investigated by Bursten and co-workers[20] with a particular emphasis on those containing six hydride ligands, which appear to be characterized by multiple M–M bonding. Theoretical studies on other selected heterobimetallic complexes that contain at least one $M(C_5H_5)(CO)_3$ unit (M = Cr, Mo or W) have also been reported.[21] It was shown that for the appropriate electron counting the $M(C_5H_5)(CO)_3$ unit is able to make a σ and a π linkage with the facing metal atom. In this paper we restrict ourselves to the question of whether a single σ Mo–Mo bond is still detectable in the unbridged piano-stool dimers of type $M_2(C_5H_5)_2L_6$ (M = Cr, Mo or W) given the long M–M separations (3.2–3.3 Å) and, if so, why this is so stretched.

Based on a previous analysis,[22] it can be stated that in $M(C_5H_5)L_4$ piano-stool monomers seven out of nine metal atomic orbitals are essentially engaged in M–L bonding interactions (basically three of them with the C_5H_5 π system and four others with the two-electron σ-donor ligands). The remaining metal orbitals, z^2 and xy based, are considered non-bonding (lone pairs), or involved in π back donation if the metal is at least d^4 and if the terminal ligands have π-acceptor capabilities.[17]

It is convenient to analyse a piano-stool dimer, such as **1**, as being formed by two interacting $M(C_5H_5)L_3$ units. This is not only a theoretical abstraction since it has been demonstrated that compounds of the type $M_2(C_5H_5)_2L_6$ (M = Cr, Mo or W) dissociate homolytically in solution.[23] The radical monomer $[Cr(C_5H_5)_2(CO)_2(PPh_3)]$ has even been isolated and studied by X-ray diffraction techniques.[24]

Fig. 2 shows a strong interaction between two metal hybrids of the individual fragments.[25] At the long imposed intermetallic distance of 3.3 Å, the σ*(Mo–Mo) level ($2b_u$) is significantly destabilized, while the corresponding in-phase σ combination ($1a_g$) falls below three of the four lone-pair combinations (see **I** and **II**, respectively). Notice also that the lone pairs are split in a sort of pairwise four-electron destabilizing interaction. In any event, a positive Mo–Mo overlap population of 0.165 is calculated while the relatively large gap (> 1.5 eV) between the

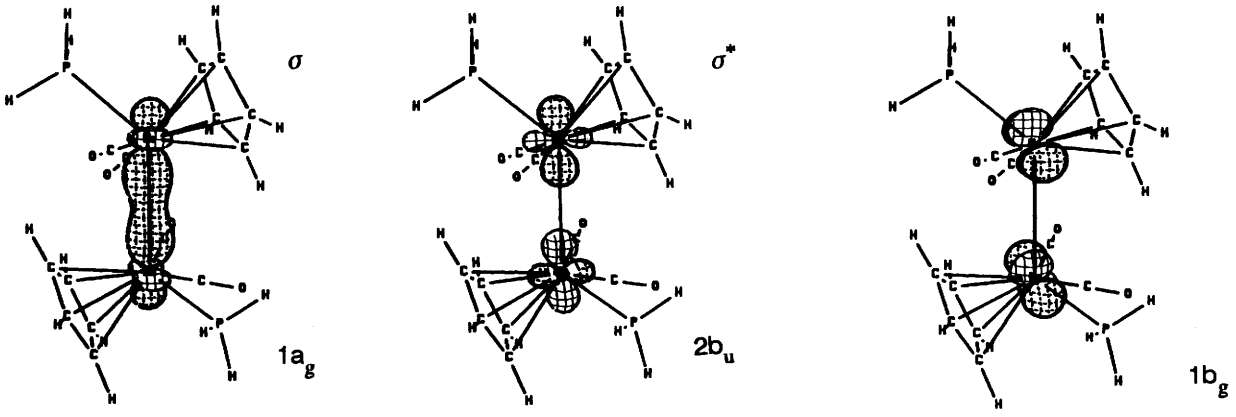

I II III

highest occupied (HOMO) and lowest unoccupied (LUMO) molecular orbitals predicts good thermodynamic stability for the dimer.

Rather than emphasizing the latter EHMO numerical results, it is better to monitor the evolution of the frontier MOs when the two $M(C_5H_5)L_3$ fragments separate, in the range 2.8–4.0 Å. The Walsh diagram in Fig. 3 suggests that direct metal–metal interactions are important for the stability of the system. Significantly, the total energy minimizes close to the experimental value of the Mo–Mo distance (*ca.* 3.3 Å). The behaviour of the single MOs shows that the electronic effects can be even more important than the steric ones in controlling the M–M separation. The total energy rises sharply only below 3.0 Å due to the short contacts between the opposite terminal ligands (C_5H_5 on one side and CO ligands on the other), whereas, near the equilibrium structure, there are contrasting electronic effects. Starting from short M–M separations, the loss of the σ-bonding MO ($1a_g$ rises) is balanced by reduced repulsions between d_π–d_π metal lone pairs, especially those carrying *xy* character (see $1b_g$ in **III**). At *ca.* 3.3 Å an energetic compromise is reached. It is noteworthy that the d_π–d_π interaction (orthogonal with respect to that in **III**) is even transformed into a Mo–Mo bonding component if, for an appropriate electron count, the π* level $2a_g$ is emptied. The existence of a π, beside a σ, M–M bond has been underlined by Sargent and Hall[21a] for heterobimetallic systems containing at least one $M(C_5H_5)L_3$ fragment.

Other features of the diagram in Fig. 3 appear rational. The empty σ* level $2b_u$ (see **I**) drops in energy but eventually it remains separated from the lower filled MOs. Accordingly electron pairing is still possible in these systems even at long distances. Remarkably, the Mo–Mo overlap population at 4.0 Å is small but still positive (= 0.076). For longer separations, however, a triplet ground state can be attained (at 4.2 Å the HOMO – LUMO gap is only 0.4 eV) and this may precede momentarily the homolytic cleavage of the dimer. The feature, well known experimentally[23] for piano-stool dimers of the Cr, Mo, W triad (chromium is the best in this respect), may be explained as follows. While σ*(M–M) drops, the σ(M–M) counterpart (the level $1a_g$) rises in energy on account of the lost Mo–Mo bonding. Gradually, the σ(M–M) character is transferred into the HOMO $2a_g$. This occurs through an avoided crossing between the levels $1a_g$ and $2a_g$ which switches the original σ and π* characters, as shown in **IV**. The closeness of σ and σ* levels for long M–M separations (small HOMO – LUMO gap) favours the higher spin multiplicity which momentarily precedes the formation of split diradicals. The different symmetries of the HOMO and the LUMO ($2a_g$ and $2b_u$, respectively) could in principle represent an obstacle to the jumping of an electron from one level to the other. At long M–M distances, however, any barrier to the free rotation of the two $M(C_5H_5)L_3$ moieties should be dismissed (see below) with consequent breakdown of the C_{2h} symmetry. Recall that electron-transfer processes are thought to occur most easily through the mechanism of avoided crossing between levels of equal symmetry.[26,27] In this particular case, the splitting of the two bonding electrons between the metals and the formation of two radicals is consistent with the σ-hybrid character of the former HOMO – LUMO levels that, moreover, become of the same symmetry.

Finally, as pointed out by Cotton and co-workers,[10d] the reciprocal orientation of the $M(C_5H_5)L_3$ moieties is apparently controlled by the M–M separation. In the piano-stool dimer $[Cr_2(\eta\text{-}C_5H_5)_2(CO)_6]$[10c] which has a M–M distance 0.06 Å longer than that of the molybdenum analogue the rotational barrier is found to be the lowest by NMR measurements. Although the EHMO method is unable to justify small differences in intermetallic distances, it suggests that the rotation of the $Mo(C_5H_5)L_3$ moieties is still hindered at 3.3 Å. In fact for certain conformations of the rotamers large four-electron repulsions (>1.2 eV) are calculated which involve oxygen lone pairs of the CO ligands bound to different metals. The M–M elongation has in comparison a much lower energy cost (as seen in Fig. 3, the stretching to 4.0 Å costs approximately 0.5 eV) and, in turn, this reduces or avoids the rotational barrier. In the Cr_2 derivative the M–C(O) distances are *ca.* 0.12 Å shorter than in the Mo_2 and W_2 analogues. Thus, the contraction of the co-ordination sphere, due to the smaller chromium radius, combined with the observed M–M elongation, decreases the rotational barrier, by avoiding short contacts between the terminal ligands. In conclusion the steric effect is certainly more important in setting the rotational barrier than in determining the stretching of the M–M bond itself.

Correlation of the MO Features with Electrochemistry.—The experimental electrochemical data can be partially interpreted in terms of the qualitative MO picture presented above. It has been shown that the system can reversibly lose one electron. The level which is half emptied is $2a_g$ (see Fig. 2). On the time-scale of cyclic voltammetry, a geometric rearrangement such as the M–M elongation must be considered very fast and fully compatible with the characteristics of the response which is typical of a reversible charge transfer. Furthermore, the removal of one electron, rather than being disruptive is, at least initially, stabilizing for the system: as mentioned, since the HOMO $2a_g$ has a partial π*(M–M) antibonding character (see **IV**), additional, although weak, π bonding between the metals is reasonably expected.

On a longer time-scale of low scan-rate voltammetry or of

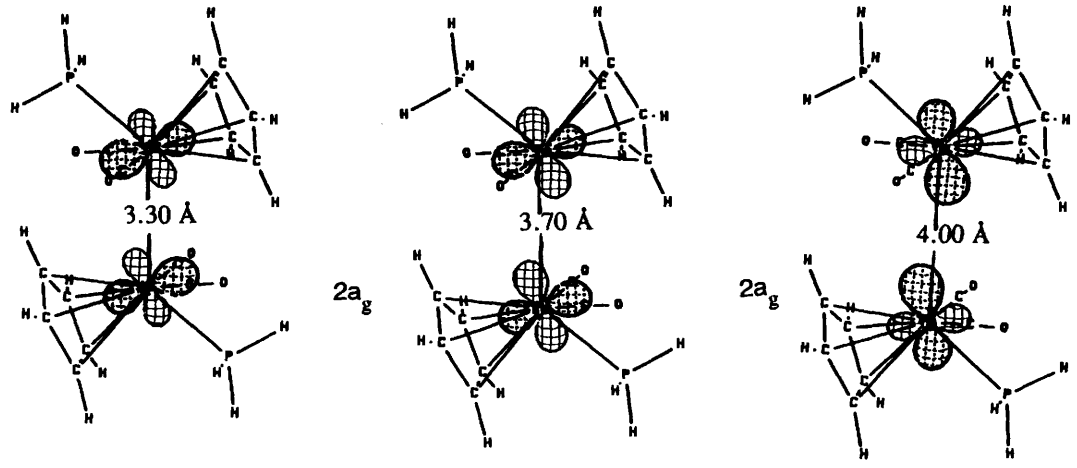

IV

exhaustive electrolysis the dimeric aggregate decompose. It cannot be excluded that the monooxidized species may be subject to Jahn–Teller effects (notice the small gap between the singly occupied MO and the lower filled levels). The associated geometric deformation may be fatal to the dimeric aggregate.

Reversible reductive processes were not feasible electrochemically, but an anionic 18-electron $Mo(C_5H_5)L_3$ species **3** was obtained from **1** *via* reaction with Na/Hg. The large HOMO–LUMO gap calculated for the geometry of **1** and the $\pi^*(CO)$ nature of the next unpopulated MO (see Fig. 3) confirm the difficulties inherent in the reduction. Only after the elongation of the Mo–Mo bond, the LUMO (now $2b_u$ with σ^* M–M character) can be populated with the consequent cleavage of the already weakened M–M bond. This can happen under drastic chemical reduction conditions or at negative potentials in an irreversible electrochemical process.[28] The cathodic behaviour of **1** is in agreement with the above arguments.

Conclusion

Although $M_2(C_5H_5)_2L_6$ piano-stool dimers have received much attention in the past,[23] the present study points out the importance of the electronic effects, probably underestimated before because of the long M–M separations. Owing to the diffuseness of the atomic orbitals of Cr, Mo and W the σ metal–metal bond is clearly operative at distances significantly longer than the sum of the atomic radii. The equilibrium distance is the result of a compromise between the direct σ attraction and the repulsion between the lone pairs of each metal. Obviously, steric effects must play their role too, but they should not be overestimated.

Similar compromises between attractive and repulsive electronic effects may also exist in compounds such as $[Mn_2(CO)_{10}]$[16] where each metal has three lone pairs (t_{2g}) which are reciprocally repulsive. In that case, however, the σ hybrid ML_5 square-pyramidal fragments are better developed than the corresponding hybrids of the $M(C_5H_5)L_3$ fragment. In addition, the environment of the terminal ligands is less demanding and ultimately the strain of the M–M bond appears less severe.

The repulsion between metal lone pairs can significantly affect the M–M bonding in clusters. One of us has recently pointed out[29] that in the system $[Fe_2(CO)_9]$ the existing σ-(Fe–Fe) attraction is overwhelmed by the repulsive interactions of some filled t_{2g} levels even if they are clearly engaged in metal–CO bridging π back donation.

In summary, M–M distances may not correlate directly with the bond order and the actual separation can often be a compromise between attractive and repulsive interactions. The latter depend in turn on the distribution of the electrons at the metals, and also the number and type of coligands present. Ultimately, the situation may vary from case to case, although the effective M–M bond order remains fixed.

Experimental

The compounds $[Mo_2(\eta\text{-}C_5H_5)_2(CO)_4]$[14] and $NC_5H_4PPh_2$-2[30] were prepared according to the published procedures; $[Mo_2(\eta\text{-}C_5H_5)_2(CO)_6]$ was purchased from Strem Chemicals. All other reagents were purchased and used as supplied. Solvents were dried by standard procedures. All experiments were performed under an atmosphere of purified nitrogen. Infrared spectra were obtained as Nujol mulls on KBr plates using a Perkin-Elmer FTIR 1720 spectrophotometer, ^1H and ^{31}P NMR spectra on a Bruker WP80-SY or a Varian Gemini-300 spectrometer. (^1H referenced to internal tetramethylsilane and ^{31}P to external 85% H_3PO_4; positive chemical shifts are for all nuclei to higher frequency). Conductivity measurements were made with a Radiometer CDM 3 conductivity meter.

Chemicals and instrumentation used in the electrochemical experiments (CH_2Cl_2) as well as the procedures followed have been described elsewhere.[31] Platinum working electrodes were used, and similar results were obtained by using either tetraethyl- or tetrabutyl-ammonium tetrafluoroborate (0.1 mol dm^{-3}) supporting electrolyte. Potential values are referred to an aqueous saturated calomel electrode (SCE).

Elemental analyses were performed by the Microanalytical Laboratory of the Organic Chemistry Institute of Milan.

Preparation of $[Mo_2(\eta\text{-}C_5H_5)_2(CO)_4(NC_5H_4PPh_2\text{-}2)_2]\cdot 2OEt_2$ **1**.—A *m*-xylene solution (15 cm^3) of $[Mo_2(\eta\text{-}C_5H_5)_2(CO)_6]$ (0.268 g, 0.546 mmol) was refluxed for 2 h; then $NC_5H_4PPh_2$-2 (0.287 g, 1.09 mmol) was added to the cooled resulting solution. Immediately the colour changed from brown to purple and a red-purple solid precipitated. Subsequently, light petroleum (50 cm^3) was added to complete the precipitation. The mother-liquor was syringed off and the red-purple precipitate washed with light petroleum and dried *in vacuo*. Yield 0.310 g (0.322 mmol), 59.1% (Found: C, 60.10; H, 4.00; N, 2.95. Calc. for $C_{48}H_{38}Mo_2N_2O_4P_2$: C, 60.00; H, 4.00; N, 2.90%).

Preparation of $[Mo(\eta\text{-}C_5H_5)(CO)_3(NC_5H_4PPh_2\text{-}2)]PF_6$ **2**.—To a dichloromethane solution (10 cm^3) of compound **1** (0.055 g, 0.057 mmol) was added $AgPF_6$ (0.029 g, 0.114 mmol) in the same solvent. Immediately, the colour changed from purple to brown-orange and silver metal deposited. The solution was filtered and purified on a Celite column (2 × 10 cm) saturated

Table 2 Atomic coordinates ($\times 10^4$) ($Å^2 \times 10^4$) with estimated standard deviations (e.s.d.s) in parentheses for the non-hydrogen atoms of complex **1**

Atom	*X/a*	*Y/b*	*Z/c*
Mo	1286(1)	97(1)	815(2)
P	2414(5)	1104(3)	1189(5)
O(1)	56(13)	1060(7)	2089(15)
O(2)	844(12)	569(7)	−2020(14)
N	1109(15)	2051(10)	−259(18)
C(1)	520(17)	718(11)	1603(21)
C(2)	918(17)	420(9)	−974(20)
C(3)	1365(25)	−1122(11)	1050(36)
C(4)	2176(24)	−908(13)	607(25)
C(5)	2944(22)	−487(11)	1595(29)
C(6)	2506(23)	−453(12)	2591(22)
C(7)	1548(23)	−804(14)	2287(31)
C(8)	1766(17)	1950(10)	950(20)
C(9)	589(20)	2657(12)	−569(25)
C(10)	771(23)	3170(15)	309(25)
C(11)	1456(21)	3070(14)	1597(26)
C(12)	1944(20)	2431(12)	1919(24)
C(13)	3335(16)	1234(10)	278(18)
C(14)	3800(17)	1862(11)	234(19)
C(15)	4535(22)	1969(14)	−409(24)
C(16)	4710(20)	1422(12)	−1114(23)
C(17)	4277(20)	807(12)	−1165(23)
C(18)	3520(17)	709(11)	−465(20)
C(19)	3382(17)	1134(9)	2838(18)
C(20)	2917(17)	1190(9)	3832(19)
C(21)	3664(20)	1188(10)	5130(22)
C(22)	4751(21)	1076(11)	5420(25)
C(23)	5169(22)	1023(11)	4470(25)
C(24)	4465(19)	1056(10)	3159(21)
C(1D)	6949(86)	2352(33)	3795(91)
C(2D)	7571(161)	1871(44)	3101(69)
O(1D)	7768(41)	1244(23)	4015(42)
C(3D)	7782(91)	588(34)	3357(62)
C(4D)	8474(62)	76(27)	4356(69)
C(5D)	6711(89)	2459(32)	2525(104)
C(6D)	7468(75)	1899(38)	2499(115)
O(2D)	7132(48)	1235(26)	2924(57)
C(7D)	8085(54)	800(40)	3645(89)
C(8D)	7734(79)	140(34)	4091(91)

with CH_2Cl_2. The resulting orange solution was reduced in volume and, by addition of light petroleum, an orange solid was obtained. It was washed with diethyl ether and vacuum dried. Yield 0.059 g (0.090 mmol), 79.0% (Found: C, 46.05; H, 3.10; N, 2.30. Calc. for $C_{24}H_{19}F_6MoNO_2P_2$: C, 46.10; H, 3.05; N, 2.25%). IR (Nujol): ν(CO) 2066, 1973, 1908; ν(PF_6) 846 cm^{-1}. Λ(MeOH) = 88 Ω^{-1} cm^2 mol^{-1}.

Reaction of Compound **1** *with Sodium Metal or Sodium Amalgam.*—A solution of compound **1** in thf was stirred vigorously with an excess of sodium metal until the purple solution changed to pale yellow (about 1 h); then the solution was filtered under nitrogen. Attempts to obtain the compound Na[Mo(η-C_5H_5)(CO)$_2$($NC_5H_4PPh_2$-2)] **3** in a pure form failed. Using sodium amalgam the reaction proceeds similarly but requires less time.

Crystallography for Compound **1**.—*Crystal data.* $C_{48}H_{38}Mo_2N_2O_4P_2 \cdot 2C_4H_{10}O$, M = 1109.91, monoclinic, space group $P2_1/c$, a = 13.218(4), b = 19.485(6), c = 11.019(4) Å, β = 110.10(2)°, U = 2665(2) $Å^3$, Z = 2, D_c = 1.382 g cm^{-3}, μ = 48.94, F(000) = 1140, λ(Cu-Kα, nickel-filtered) = 1.541 838 Å.

Data collection, structure determination and refinement. Even if of very small size, crystals of compound **1** suitable for X-ray analysis were obtained from diethyl ether solutions. A crystal of approximate dimensions 0.10 × 0.12 × 0.20 mm was used for the data collection on a Siemens AED single-crystal diffractometer. Unit-cell parameters were obtained by least-squares refinement of the θ values of 26 accurately measured reflections (θ 18–29°). Data were collected at room temperature (22 °C) using nickel-filtered Cu-Kα radiation and θ–2θ scans. The reflections were collected with a variable scan speed of 3–12° min^{-1} and a scan width from (θ − 0.65)° to (θ + 0.65 + 0.142 tan θ)°. A decay of about 25% of the initial intensity of one standard reflection, measured every 50 reflections as a general check on crystal and instrument stability, was observed during the data collection. The individual profiles were analysed according to Lehmann and Larsen.[32] A total of 4106 reflections were measured in the range 2θ 6–120°. The intensities were corrected for Lorentz and polarization effects, and for absorption (maximum and minimum values of the transmission factors 1.243 and 0.878).[33] Only the observed reflections [1195, having $I > 2\sigma(I)$] were used in the structure solution and refinement.

The structure was solved by Patterson and Fourier methods, and refined by full-matrix least squares first with isotropic thermal parameters and in the last cycles with anisotropic thermal parameters only for the Mo and P atoms, for the atoms of the carbonyl groups and for the carbon atoms of the cyclopentadienyl ring. The N atom in the ligand $NC_5H_4PPh_2$-2 was assigned by evaluating the isotropic thermal parameters, the bond lengths, the intramolecular contacts and the R values in seven different trial refinements. In the first one all of the atoms of the three six-membered rings were treated as carbon, then the N heteroatom was tested in each of the two possible positions within the different rings. The ultimate choice was made also by considering that one of the shortest intermolecular contacts [3.26 Å from the carbonyl atom C(2)] suits better a N heteroatom than a CH group. In addition, no intra- or inter-molecular H ··· H contact is <2.3 Å for the given assignment of the N atom. In the final ΔF map a diethyl ether molecule of solvation was found disordered and distributed in two positions of equal occupancy factor 0.5. All hydrogen atoms, except those of the solvent molecule, were placed at their geometrically calculated positions (C–H 1.00 Å) and refined 'riding' on the corresponding carbon atoms. The final cycles of refinement were carried out on the basis of 213 variables; after the last cycles, no parameters shifted by more than 0.45 e.s.d. The biggest remaining peak in the final difference map was equivalent to about 0.85 e $Å^{-3}$. A weighting scheme $w = K[\sigma^2(F_o) + gF_o^2]^{-1}$ was used in the last cycles of refinement; at convergence K and g were 0.616 and 0.0243 respectively. Final R and R' values were 0.0698 and 0.0917 respectively. The SHELX 76 and SHELXS 86 systems of computer programs were used.[34] Atomic scattering factors, corrected for anomalous dispersion, were taken from ref. 35. Final atomic coordinates for the non-hydrogen atoms are given in Table 2. All calculations were carried out on the CRAY X-MP/48 computer of the Centro di Calcolo Elettronico Interuniversitario dell'Italia Nord-Orientale, Bologna and on the GOULD POWERNODE 6040 of the Centro di Studio per la Strutturistica Diffrattometrica del C.N.R., Parma.

Additional material available from the Cambridge Crystallographic Data Centre comprises H-atom coordinates, thermal parameters and remaining bond lengths and angles.

Computational Details.—All of the calculations were of the extended-Hückel type[12] with a modified version of the Wolfsberg–Helmholz formula. The atomic parameters for Mo were taken from ref. 36. The models used have the following geometrical features: C–C distances (in C_5H_5) 1.40, C–O 1.10, Mo–CE 2.0 Å (CE=C_5H_5 centroid). The other structural parameters (*e.g.* Mo–CO, Mo–PH_3 distances, the average angles, *etc.*) were fixed at the values of the experimental structure of compound **1**.

Acknowledgements

We thank the Consiglio Nazionale delle Ricerche (Progetto Finalizzato Chimica Fine II) and the Italian Ministero dell'Università e della Ricerca Scientifica e Tecnologica for financial support.

References

1 M. D. Curtis, *Polyhedron*, 1987, **6**, 759.
2 G. Bruno, S. Lo Schiavo, E. Rotondo, C. G. Arena and F. Faraone, *Organometallics*, 1989, **8**, 886.
3 E. Rotondo, S. Lo Schiavo, G. Bruno, C. G. Arena, R. Gobetto and F. Faraone, *Inorg. Chem.*, 1989, **28**, 2944.
4 S. Lo Schiavo, E. Rotondo, G. Bruno and F. Faraone, *Organometallics*, 1991, **10**, 1613; C. G. Arena, E. Rotondo, F. Faraone, M. Lanfranchi and A. Tiripicchio, *Organometallics*, 1991, **10**, 3877.
5 P. E. Garrow, *Chem. Rev.*, 1981, **81**, 256; R. Poli, S. T. Krueger, F. Abugideri, B. S. Haggerty and A. L. Reinghold, *Organometallics*, 1991, **10**, 3041.
6 S. Lo Schiavo, F. Faraone, M. Lanfranchi and A. Tiripicchio, *J. Organomet. Chem.*, 1990, **387**, 357.
7 R. J. Klingler, W. Butler and M. D. Curtis, *J. Am. Chem. Soc.*, 1975, **97**, 3535.
8 R. J. Haines and C. R. Nolte, *J. Organomet. Chem.*, 1970, **24**, 725.
9 R. J. Haines, R. S. Nyholm and M. H. B. Stiddard, *J. Chem. Soc. A*, 1968, 43.
10 (*a*) F. C. Wilson and D. P. Shoemaker, *J. Chem. Phys.*, 1957, **27**, 809; (*b*) R. D. Adams and F. A. Cotton, *Inorg. Chim. Acta*, 1973, **7**, 153; (*c*) R. D. Adams, D. M. Collins and F. A. Cotton, *J. Am. Chem. Soc.*, 1974, **96**, 749; (*d*) R. D. Adams, D. M. Collins and F. A. Cotton, *Inorg. Chem.*, 1974, **5**, 1086.
11 C. Mealli and D. M. Proserpio, *J. Chem. Educ.*, 1990, **67**, 399.
12 R. Hoffmann and W. N. Lipscombe, *J. Chem. Phys.*, 1962, **36**, 2179, 3489; R. Hoffmann, *J. Chem. Phys.*, 1963, **39**, 1397.
13 R. Hoffmann, H. Fujimoto, H. J. R. Swenson and C. C. Wan, *J. Am. Chem. Soc.*, 1973, **95**, 7644; R. Hoffmann and H. Fujimoto, *J. Phys. Chem.*, 1974, **78**, 1167.
14 D. S. Ginley and M. S. Wrighton, *J. Am. Chem. Soc.*, 1975, **97**, 3533.
15 A. F. Wells, *Structural Inorganic Chemistry*, Clarendon Press, Oxford, 1975.
16 M. R. Churchill, K. N. Amoh and H. J. Wasserman, *Inorg. Chem.*, 1981, **20**, 1609; M. Martin, B. Rees and A. Mitschler, *Acta Crystallogr., Sect. B*, 1982, **38**, 6.
17 R. Poli, *Organometallics*, 1990, **9**, 1892.
18 G. Bontempelli, F. Magno, G. A. Mazzocchin and R. Seeber, *Ann. Chim. (Rome)*, 1989, **79**, 103.
19 R. S. Nicholson and I. Shain, *Anal. Chem.*, 1964, **36**, 706.
20 B. E. Bursten, R. H. Cayton and M. G. Gatter, *Organometallics*, 1988, **7**, 1342; B. E. Bursten and R. H. Cayton, *Organometallics*, 1988, **7**, 1349.
21 (*a*) A. L. Sargent and M. B. Hall, *J. Am. Chem. Soc.*, 1989, **111**, 1563; (*b*) L. Carlton, W. E. Lindsell, K. J. McCullough and P. N. Preston, *Organometallics*, 1985, **4**, 1138.
22 P. Kubacek, R. Hoffmann and Z. Havlas, *Organometallics*, 1982, **1**, 180.
23 M. C. Baird, *Chem. Rev.*, 1988, **88**, 1217 and refs. therein.
24 N. A. Cooley, K. A. Watson, S. Fortier and M. C. Baird, *Organometallics*, 1986, **5**, 2563.
25 M. Elian and R. Hoffmann, *Inorg. Chem.*, 1975, **14**, 1058; see also T. A. Albright, J. K. Burdett and M. H. Whangbo, *Orbital Interactions in Chemistry*, Wiley, New York, 1985.
26 L. Salem, *Electrons in Chemical Reactions: First Principles*, Wiley-Interscience, New York, 1982.
27 C. Mealli, M. Sabat and L. G. Marzilli, *J. Am. Chem. Soc.*, 1987, **109**, 1593.
28 A. A. Vlcek, *Prog. Inorg. Chem.*, 1963, **5**, 211.
29 C. Mealli and D. M. Proserpio, *J. Organomet. Chem.*, 1990, **386**, 203.
30 F. G. Mann and J. Watson, *J. Org. Chem.*, 1948, **13**, 502.
31 R. Seeber, G. Minghetti, M. I. Pilo, G. Banditelli and S. Zamponi, *J. Organomet. Chem.*, 1991, **402**, 413.
32 M. S. Lehmann and F. K. Larsen, *Acta Crystallogr., Sect. A*, 1974, **30**, 580.
33 N. Walker and D. Stuart, *Acta Crystallogr., Sect. A*, 1983, **39**, 158; F. Ugozzoli, *Comput. Chem.*, 1987, **11**, 109.
34 G. M. Sheldrick, SHELX 76, Program for crystal structure determination, University of Cambridge, 1976; SHELXS 86, Program for the solution of crystal structures, University of Göttingen, 1986.
35 *International Tables for X-Ray Crystallography*, Kynoch Press, Birmingham, 1974, vol. 4.
36 R. H. Summerville and R. Hoffmann, *J. Am. Chem. Soc.*, 1976, **98**, 7240.

Received 25*th November* 1991; *Paper* 1/05977G